

Introduction

The Earth's climate, past and future, is not static; it changes in response to both natural and anthropogenic drivers. There is evidence that anthropogenic emissions of greenhouse gases (GHGs) have altered the large-scale patterns of temperature and other variables over the twentieth century. GHGs such as carbon dioxide (CO₂) have increased by 46% and methane (CH₄) by 157% between 1750 to 2018 globally. CH₄ is the second-largest greenhouse gas in terms of radiative forcing. However, studies on the concentration, sources, and climatic implications of CH₄ is limited in South Asia's Eastern Himalayan Region (EHR), which is a vulnerable area to climate change. CH₄ is one of the dominant trace gases in the study region. Therefore, multiple datasets have been used to quantitatively study the global/regional spatial-temporal distribution of CH₄ and its impact on radiative forcing and surface temperature.

Methodology

1. Copernicus Atmospheric Monitor Service (CAMS) Greenhouse Gases Flux Inversions monthly average CH₄ emission data from 1990-2016.
2. The new version of Emissions Database for Global Atmospheric Research (EDGARv7) emission inventory data from 1970-2019.
3. CMIP5 models with Representative Concentration Pathway(RCP 8.5) are used to represent the past, present and future CH₄ emission.
4. MODIS (both Aqua and Terra) LULC product MCD12Q1 v006, provides yearly land cover data at the spatial resolution of 500m.
5. The European Space Agency (ESA) Greenhouse Gas Climate Change Initiative homogenized the SCIAMACHY and GOSAT datasets and produced a long-term CH₄ dataset for climate applications.
6. The radiative forcing (RF) due to methane (CH₄) is calculated using the following expressions used in Etminan et al. (2016).

$$RF = [a_3\bar{M} + b_3\bar{N} + 0.043] (\sqrt{M} - \sqrt{M_0}) \quad \text{----- 1}$$

Where,

$$a_3 = -1.3 \times 10^{-6} \text{ Wm}^{-2} \text{ppb}^{-1}$$

$$b_3 = -8.2 \times 10^{-6} \text{ Wm}^{-2} \text{ppb}^{-1}$$

$$\bar{M} = 0.5 (M + M_0)$$

$$\bar{N} = 0.5 (N + N_0)$$

$$M_0 = \text{initial concentration of CH}_4$$

$$M = \text{final concentration of CH}_4$$

$$N_0 = \text{initial concentration of N}_2\text{O}$$

$$N = \text{final concentration of N}_2\text{O}$$

The change in surface temperature due to methane as a function of radiative forcing is derived from equation 2 (Huntingford & Cox, 2000).

$$-\kappa \frac{\partial \Delta T_0}{\partial z} = \Delta H_0 = \frac{\Delta Q(t)}{f} - \Delta T_0 \left[\frac{(1-f)\lambda_1 v}{f} + \lambda_0 \right] \quad \text{----- 2}$$

ACKNOWLEDGEMENTS

ICIMOD and its Regional Member Countries gratefully acknowledge the generous support of Austria, Norway, Sweden and Switzerland for core and programme funding, and Australia, Canada's International Development Research Centre, the European Union, Finland, Germany, the United Kingdom, the United States of America, and the World Bank for project funding. The views and interpretations in this publication are those of the authors and are not necessarily attributable to ICIMOD.

REFERENCES

- Etminan M, Myhre G, Highwood EJ, Shine KP (2016). Radiative forcing of carbon dioxide, methane, and nitrous oxide: a significant revision of the methane radiative forcing. *Geophys Res Lett* 43:12614–12623. <https://doi.org/10.1002/2016GL071930>
- Huntingford C, Cox PM (2000). An analogue model to derive additional climate change scenarios from existing GCM simulations. *Clim Dyn* 16:575–586. <https://doi.org/10.1007/s003820000067>

Results

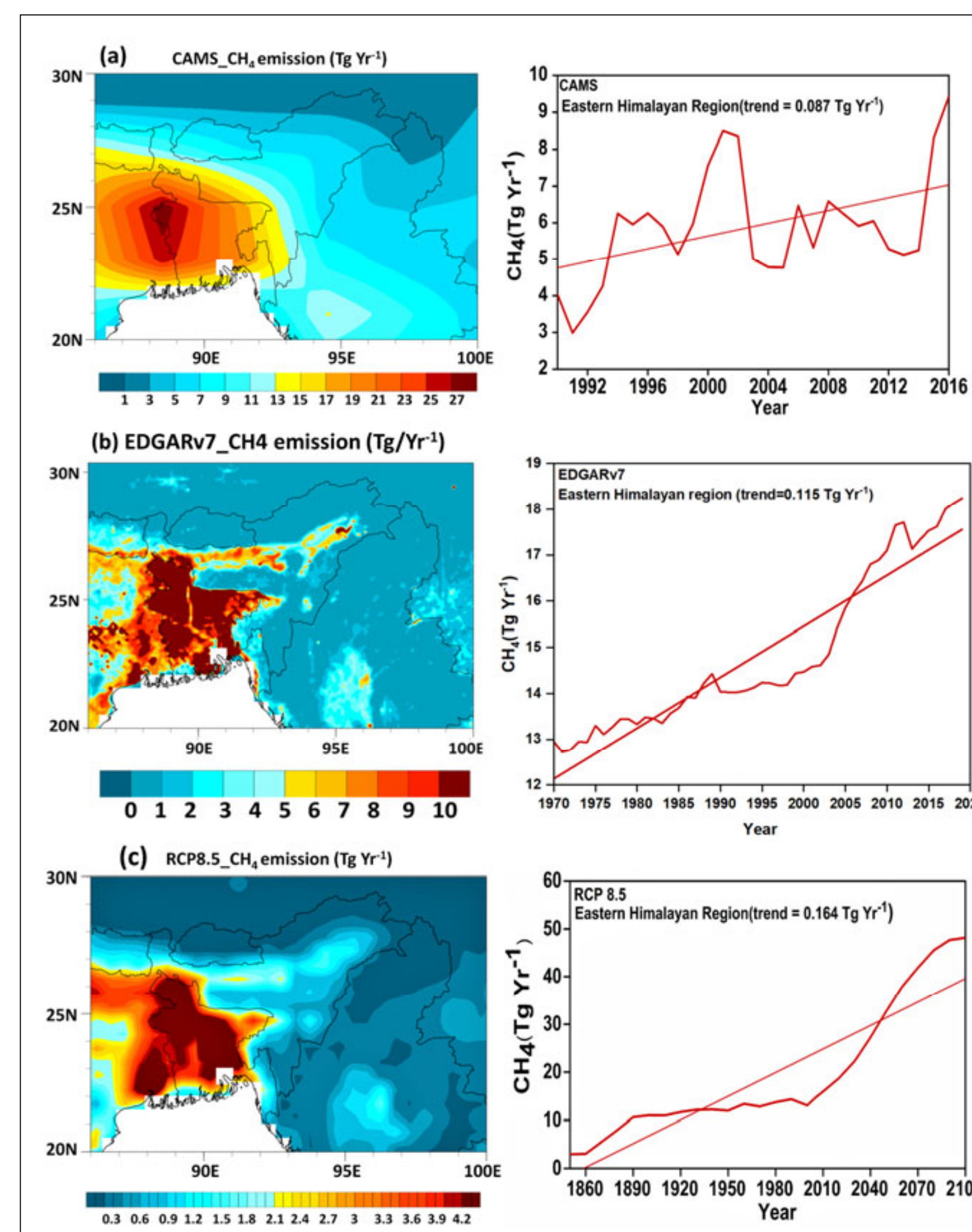


FIGURE 1: CH₄ emission maps and time-series over the EHR using (a) CAMS, (b) EDGARv7, and (c) RCP 8.5 emission datasets.

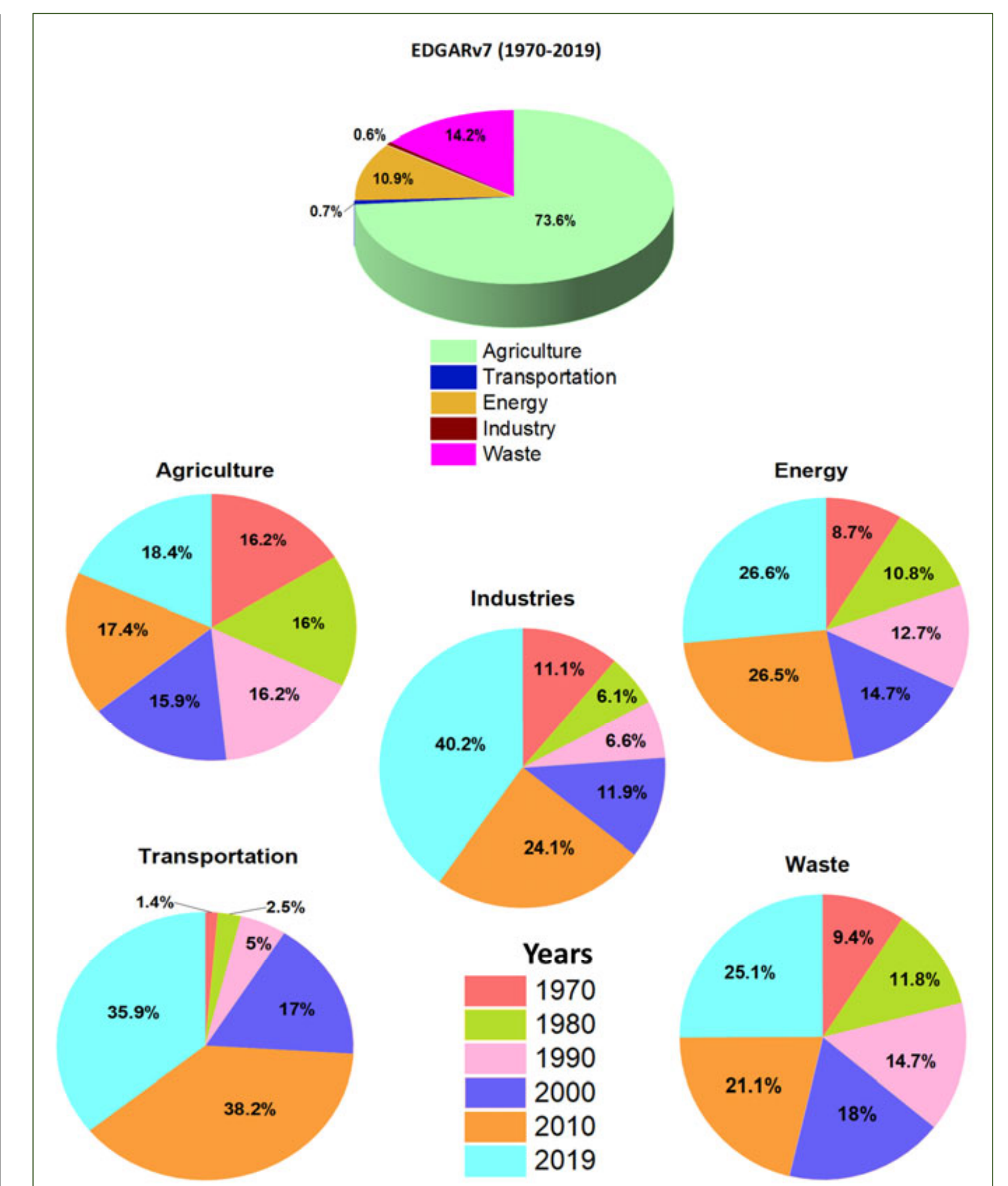


FIGURE 2: The anthropogenic sectors contributing to total CH₄ emissions taken from EDGAR version7 for 50 years.

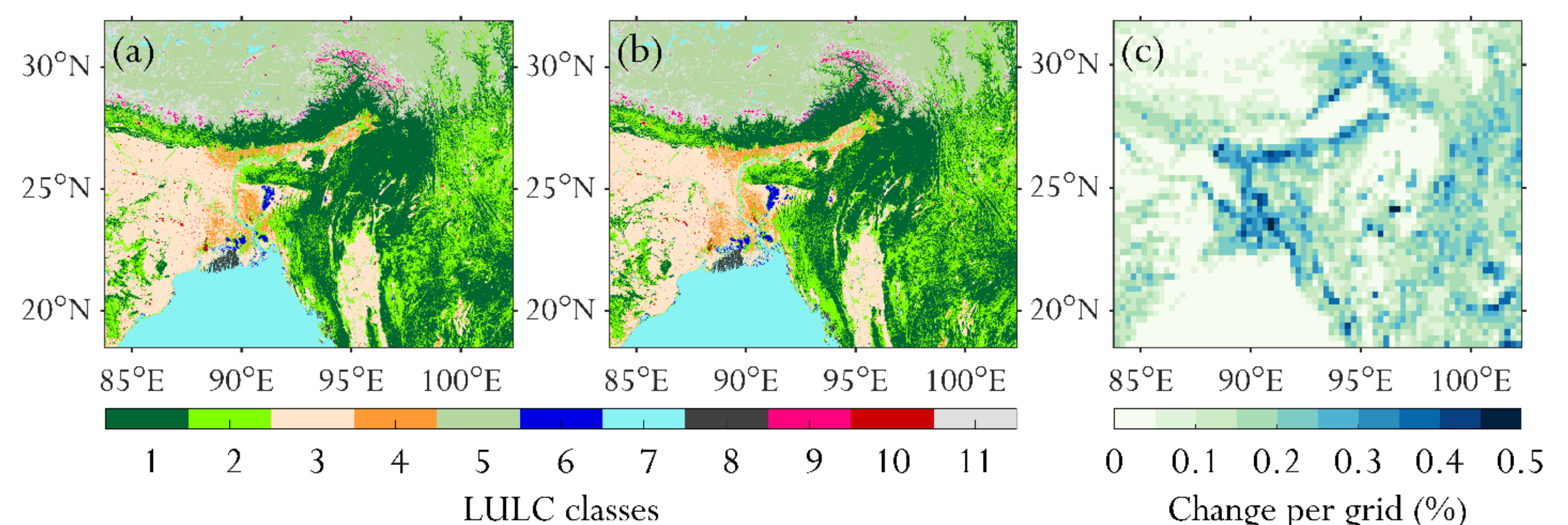


FIGURE 3: Land Use and Land Cover during (a) 2001 (b) 2018 (c) Change between 2001 and 2018(%). The numbers in the label bars represent LULC classes: 1-Forests, 2-Grasslands, 3-Croplands, 4-Cropland/Natural Vegetation, 5-Shrublands (including Tundra Shrubs), 6-Wetlands, 7-Water Bodies, 8-Mangroves, 9-Snow and Ice, 10-Urban/Built-up lands, and 11-Barren lands.

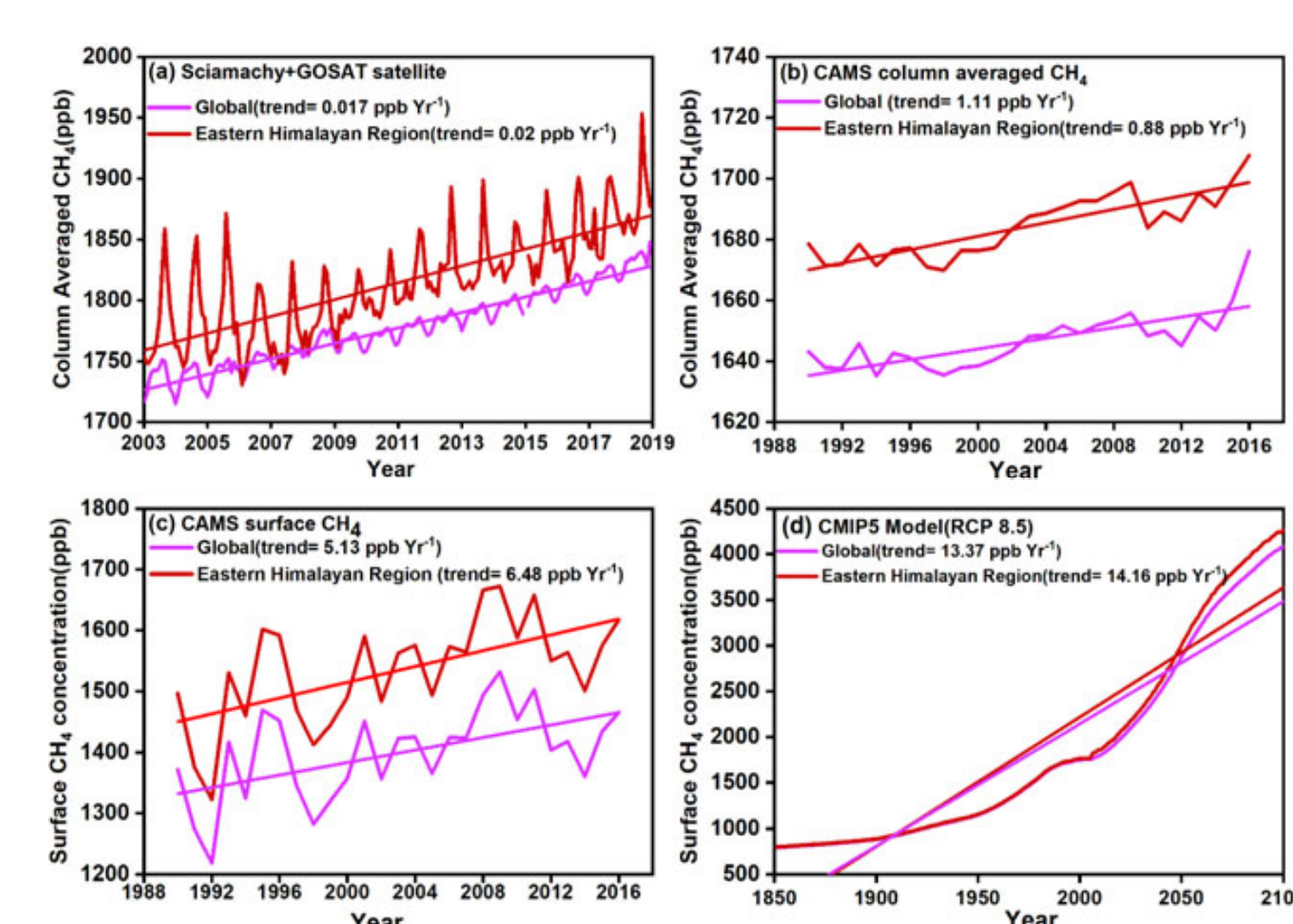


FIGURE 4: Interannual variation of CH₄ concentration over the globe and the EHR using satellite, reanalysis, and model datasets.

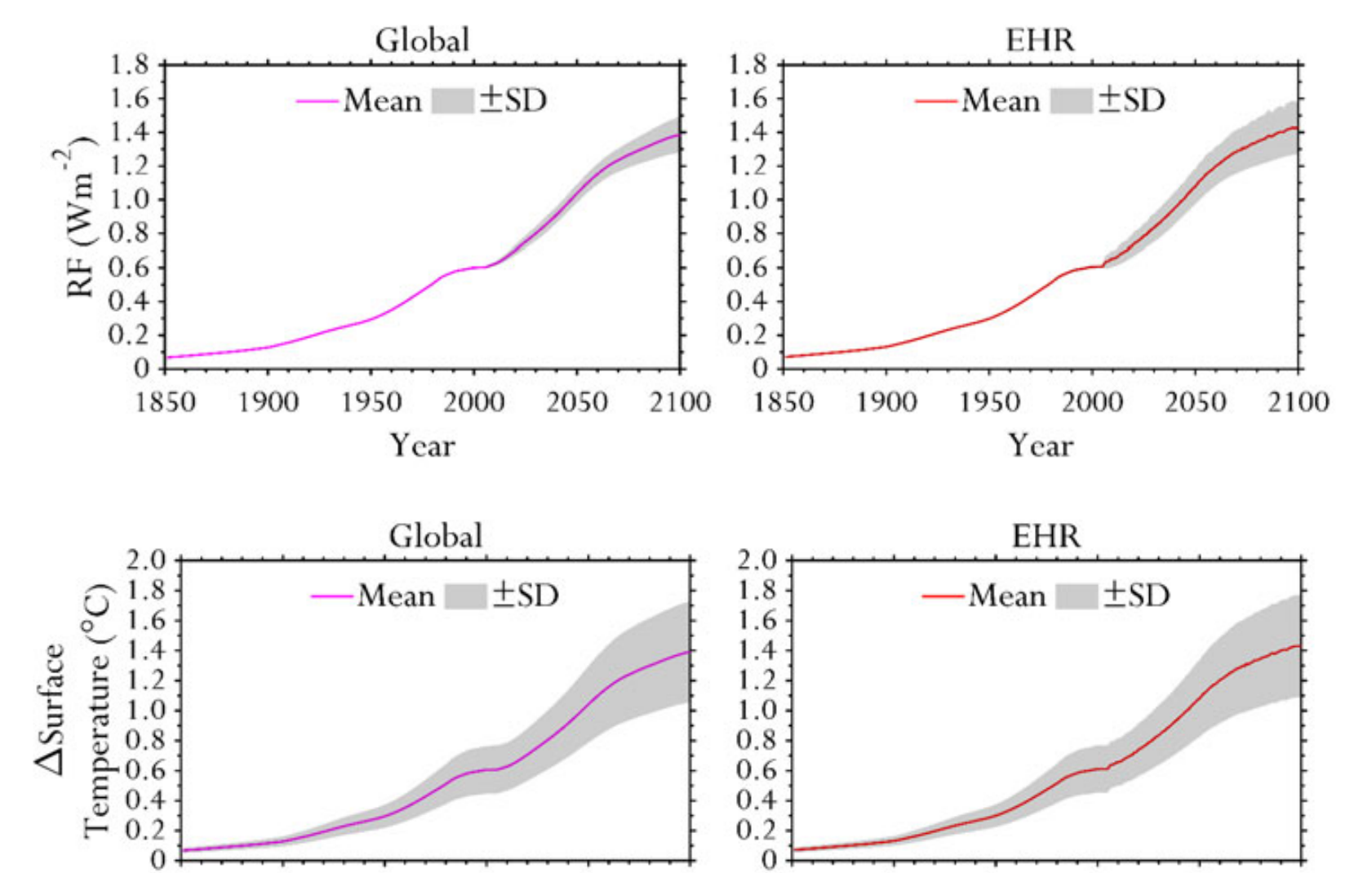


FIGURE 5: Estimated global and regional CH₄ radiative forcing (RF) and the resultant change in the surface temperature due to CH₄ as a function of RF 1851-2100 based on CMIP5 data.

Conclusions

- CH₄ emissions estimated over the study location show an increasing trend from CAMS ~0.087 Tg Yr⁻¹, EDGARv7 ~0.11 Tg Yr⁻¹, and RCP8.5 ~0.16 Tg Yr⁻¹.
- Based on the RCP8.5 future emissions scenario, CH₄ show an increasing trend over the EHR, increasing more than 2-fold (32.7 Tg CH₄ Yr⁻¹) by 2050 and up to 3-fold (~48.2 Tg CH₄ Yr⁻¹) by 2100 compared to the year 2000 (14.6 Tg CH₄ Yr⁻¹).
- The rate of enhancement of CH₄ emissions from agriculture, energy, industries, transportation, and waste increased by 18.4%, 26.6%, 40.2%, 35.9%, 25.1% in 2019 compared to 1970.
- We observed an increase of 0.098% and 0.033% in total wetland and water bodies coverage, respectively and found ~0.42% of forest cover loss, which were mostly converted to cropland in the study area.
- The interannual CH₄ peaks have been observed in all the datasets since 2007. All results show a statistically significant (p<0.05) increasing trend of CH₄ concentrations, which is associated with increasing emissions from anthropogenic sources.
- The estimated CH₄-induced temperature change as a function of change in the radiative forcing exhibits an increasing trend at the rate of 0.0036°C Yr⁻¹ worldwide and 0.0062°C Yr⁻¹ over the EHR.

¹International Centre for Integrated Mountain Development (ICIMOD), Kathmandu, Nepal; ²Centre of Excellence in Disaster Mitigation and Management, Indian Institute of Technology Roorkee, Uttarakhand, India; ³Centre for Atmospheric Studies, Dibrugarh University, India